Functional differential equations in sustainable forest harvesting *

Oscar García †

Abstract

The sustainability of harvesting a given constant volume in a simplified forest model is studied. Depending of the initial age distribution, the cut can lead to the forest exhaustion, or the forest may tend asymptotically to a steady-state uniform age distribution. A continuous model is formulated in terms of various kinds of partial differential equations, delay differential equations, and non-linear integral equations. Equilibrium solutions and their stability properties are determined. Discrete models are also obtained, both by direct reasoning and as approximations to the continuous case. These are used for simulation and graphical exploration of the system behavior. In addition, contrasting various discrete and continuous versions was found useful in clarifying some issues, in particular, ambiguity/redundancy problems in the relation between integral equations and delay differential equations derived from them. The basic problem of evaluating sustainability for an initial distribution remains unsolved, however. Further progress is linked to the asymptotic properties of a second-order recurrence relationship. It is hoped that the interplay between the theory of functional differential equations and this concrete and easily interpretable problem in forest management might prove fruitful in both fields.

*Working Paper. Royal Veterinary and Agricultural University, Department of Economics and Natural Resources, Unit of Forestry. July 1997.

†KVL, Sektion for Skovbrug, Thorvaldsensvej 57, DK-1871 Frederiksberg C, Denmark. `og@kvl.dk`

1 Introduction

Among mathematicians there is currently a great deal of interest in delay differential equations (DDEs.) Some simplified but fundamental forest management models can be formulated in terms of DDEs or non-linear integral equations (both DDEs and integral equations seem to be included under the more general label of *functional differential equations*.) Putting these facts together may benefit both disciplines. Perhaps FDE specialists might contribute to solving long-standing open questions that block progress in the understanding and optimization of forest management strategies. On the other hand, the forest models described here can help mathematical developments, providing concrete physical interpretations to guide intuition and suggest new approaches.

Forest management planning can be approached from two different directions. Practical real-life problems are confronted with simulation and Mathematical Programming techniques, mostly Linear Programming and Mixed Integer Programming (Clutter et al., 1983; Leuschner, 1990; García, 1990). In many instances reasonably realistic models can be solved with current hardware and software, but there is always pressure to increase resolution levels and computational efficiency, even more so when integer constraints or nonlinearities are involved. On a theoretical level, highly simplified models are studied analytically, hopefully improving our basic understanding of the main issues (Johansson & Lofgren, 1985). Present practical methods can to a large extent be characterized as "brute force"; realizing the potential of fully exploiting the special problem structure would depend of further advances in the theoretical front (García, 1990).

Unfortunately, analytical developments in forest planning have not progressed as much as one would like. The optimization of independent forest stands, where over-all production level does not affect costs and revenues, was solved by Faustmann (1849) long before modern investment theory catched up with him. The steady-state solution for a level of production (*yield*) that remains constant over time, the so-called "normal forest", is older still (Section 2.) Further embellishments and extensions, such as fluctuating prices and considerations of risk, are numerous, often utilizing sophisticated Control Theory mathematics (e. g., Johansson & Lofgren, 1985). However, the logical next step of obtaining a constant yield starting from an arbitrary, not steady-state age distribution, is not satisfactorily resolved. This is the problem considered here, as a stepping stone to more practi-

cally interesting problems involving non-decreasing yields, capacity expansion costs, etc.

The next section describes the forestry problem, followed by a more precise mathematical statement in continuous time. Several alternative formulations are shown. Then some equilibrium properties of the system are discussed. Finally, discrete model versions and some simulation results are presented.

2 The problem: Forest regulation and the normal forest

Let the forest at time t be characterized by its age distribution $F_t(x)$ giving the area with ages less than or equal to x. Without loss of generality, we shall assume that the total forest area is 1. The volume yield per unit area is given by a nondecreasing function of age $g(x)$ with $g(0) = 0$ (see, for example, Figure 1.) There is a rate of volume harvesting $v(t)$, taken from the oldest ages, with the cleared land being regenerated immediately.

The classic *normal forest* theory, dating from the early 19th century, deals with the steady-state situation. A normal or *fully regulated* forest has a uniform age distribution, with equal areas for all ages between 0 and the oldest age r. The distribution is maintained by cutting all stands when they reach the *rotation age* r. It is easy to see that the area is harvested and regenerated at a rate $1/r$, producing in perpetuity an even volume flow or *sustained yield* equal to the "mean annual increment" (MAI) for the rotation age, $v = g(r)/r$. The maximum sustainable yield is obtained with the rotation of maximum MAI (Clutter et al., 1983; Leuschner, 1990)

The forest behavior outside the steady state is much less well understood. It is clear that a constant area harvesting rate (a forest regulation method known as *area control*) perpetuates the age distribution except for a cyclical shift, and produces a fluctuating volume yield. We shall examine here the effects of a constant volume harvesting rate $v(t) = v$. Traditionally this is known as *volume control* and, under certain circumstances, is supposed to lead to a normal forest. The dynamics of a forest under a constant volume cut has been extensively investigated through simulation by Allison (Allison, 1978; Clutter et al., 1983), in connection with measures of forest "maturity".

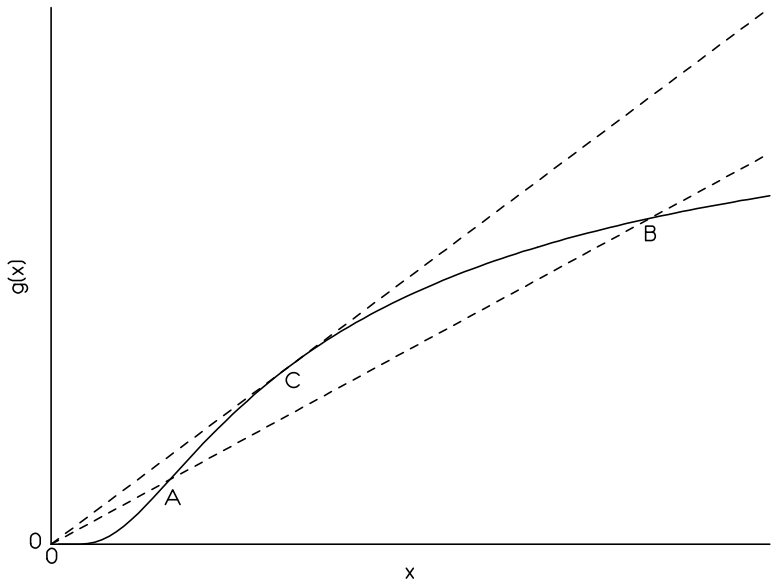

Figure 1: Example yield curve. Points A, B and C show possible normal forest rotations for volume harvesting rates equal to the line slopes

Actually, both Allison and classic forest regulation deal with a discrete version of the model, with discrete age classes and annual or periodic harvesting. Initially, we shall work mostly in continuous-time. It might be possible to include the discrete-time formulation by using appropriate stepped functions for $F(x)$ and $g(x)$. Often it is be convenient to assume that the functions are strictly increasing; this could be assured by giving an arbitrarily small slope ϵ to the steps, and taking limits at the end. Similarly, differentiability can be achieved by an infinitesimal rounding of the step corners. I shall just ignore the messy details, and assume functions as well-behaved as necessary in any particular instance. Later, in Section 5, a different discretization that may be more convenient for certain uses is introduced.

We may describe some "known" (or at least plausible) characteristics of the process; formal proofs will be provided later. If a forest with an arbitrary initial age distribution is harvested at a constant rate v, two possible outcomes have been observed. If v is too high and/or there is no enough area in older ages, at some point the forest is exhausted, that is, the yield v is not sustainable. The cutting age $r(t) = F_t^{-1}(1)$ fluctuates, finally reaching

zero[1]. Otherwise, the forest eventually approaches a steady-state uniform distribution (a normal forest.) From our previous discussion of the normal forest, it follows that the equilibrium cutting age must satisfy $g(r) = vr$. This corresponds to the intersections of the yield curve $g(x)$ and a line with slope v (Figure 1). With a typical sigmoidal yield curve there are in general two possible solutions, shown as A and B. However, A is an unstable equilibrium point, and most simulations will either exhaust the forest or converge to B. It is clear that the maximum possible sustainable v for any forest equals the maximum MAI (point C.)

It is also conceivable that some combinations of initial distribution and harvesting rate might result in neither exhaustion nor a uniform steady state. The cutting age $r(t)$ might approach a limit cycle, oscillating indefinitely without ever becoming constant. In fact, this possibility cannot be ruled out by the simulation results; apart from numerical accuracy issues, convergence in some instances is extremely slow. Determining without resorting to simulation if a given distribution will sustain or "crash" is still an open question, but we show below that limit cycles are not possible.

3 Mathematical formulations

3.1 Partial differential equations

We want to find how the age distribution $F_t(x) \equiv F(t, x)$ changes over time. Let $\mathrm{d}s$ be the area cut (from the oldest ages) and regenerated during a time interval $\mathrm{d}t$. Age x at time t becomes age $x + \mathrm{d}t$ at time $t + \mathrm{d}t$. Therefore, the area of ages $\leq x + \mathrm{d}t$ at time $t + \mathrm{d}t$ equals the area of ages $\leq x$ at time t plus the area $\mathrm{d}s$ that was regenerated between t and $t + \mathrm{d}t$:

$$F(t + \mathrm{d}t, x + \mathrm{d}t) = F(t, x) + \mathrm{d}s$$

(see Figure 2.) Using a Taylor series on the left-hand side this becomes, for $\mathrm{d}t \to 0$,

$$\frac{\partial F(t,x)}{\partial t} + \frac{\partial F(t,x)}{\partial x} = \frac{\mathrm{d}s}{\mathrm{d}t} \ .$$

[1] As in the normal forest, it is common to refer to the cutting or felling age as "rotation", although the appropriateness of the term in this instance may be questionable. I will continue denoting it by r

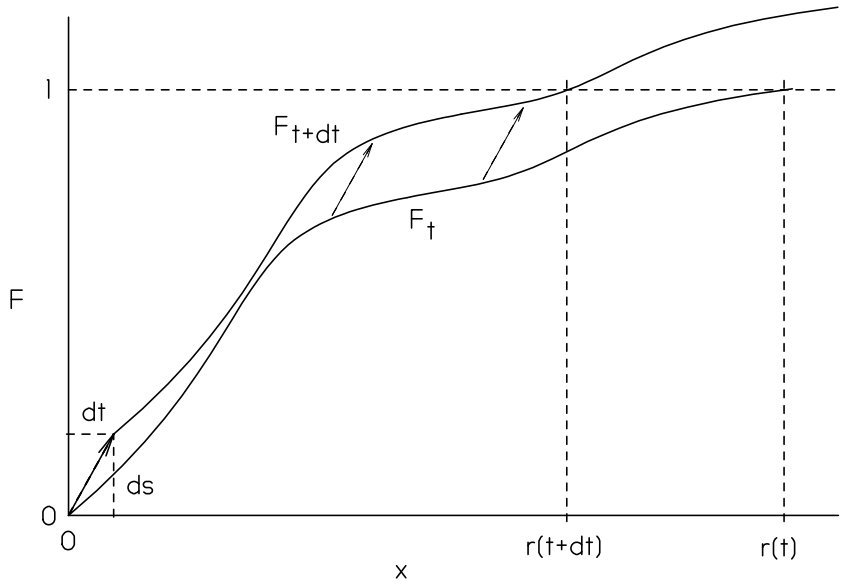

Figure 2: Evolution of the age distribution

The area cut is the volume cut divided by the yield (assumed positive). That is, for a small $\mathrm{d}t$,

$$\mathrm{d}s = \frac{v\mathrm{d}t}{g[r(t)]} \,, \tag{1}$$

where $r(t) = F_t^{-1}(1) \equiv F^{-1}(t,1)$ is the cutting age. Finally,

$$\frac{\partial F(t,x)}{\partial t} + \frac{\partial F(t,x)}{\partial x} = \frac{v}{g[F^{-1}(t,1)]} \,. \tag{2}$$

A slightly better-looking relationship is obtained for the inverse distribution function $F_t^{-1}(p) \equiv H_t(p) \equiv H(t,p)$, assuming that $F_t(x)$ is strictly increasing. Using a similar argument (turn around Figure 2), we get

$$H(t+\mathrm{d}t, p+\mathrm{d}s) = H(t,p) + \mathrm{d}t \,,$$

$$\frac{\partial H(t,p)}{\partial t} + \frac{\partial H(t,p)}{\partial p}\frac{\mathrm{d}s}{\mathrm{d}t} = 1 \,,$$

or

$$v\frac{\partial H(t,p)}{\partial t} = g[H(t,1)][1 - \frac{\partial H(t,p)}{\partial t}] \,. \tag{3}$$

This type of partial differential equation is non-standard in that it contains a "cross-section" $H(t,1)$ of the independent function. It is not clear to me how to proceed further, so we take a different tack.

3.2 Delay differential equations: The wandering coordinates trick

It is clear from Figure 2 that for small time intervals most of the distribution function remains the same, it just gets shifted. So, instead of shifting F, let us try keeping the curve fixed and shift the axes. Figure 3 shows the same sequence of distributions from Figure 2, but with two sets of coordinates.

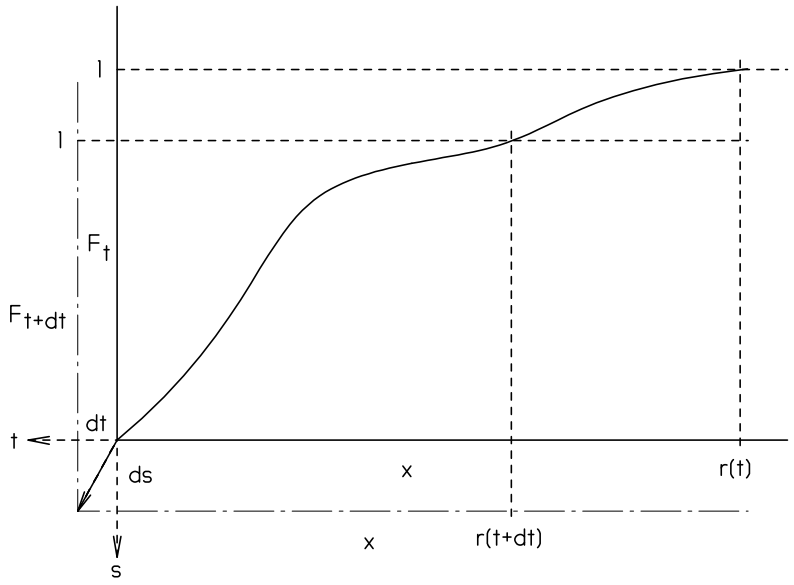

Figure 3: Moving coordinates

The origin of coordinates moves along a curve of s over t (or t over s) determined by equation (1). Doing so it determines $F_t(x)$ for any future t as an appropriate segment of that curve. For a more conventional view of the s-over-t trajectory, turn the page around 180 degrees. Again, things turn out neater with the inverse distribution, so we swap the axes after the rotation (Figure 4, where to simplify we show the situation at $t = 0$.)

Now we can write the equation for the trajectory of t over s in that Figure.

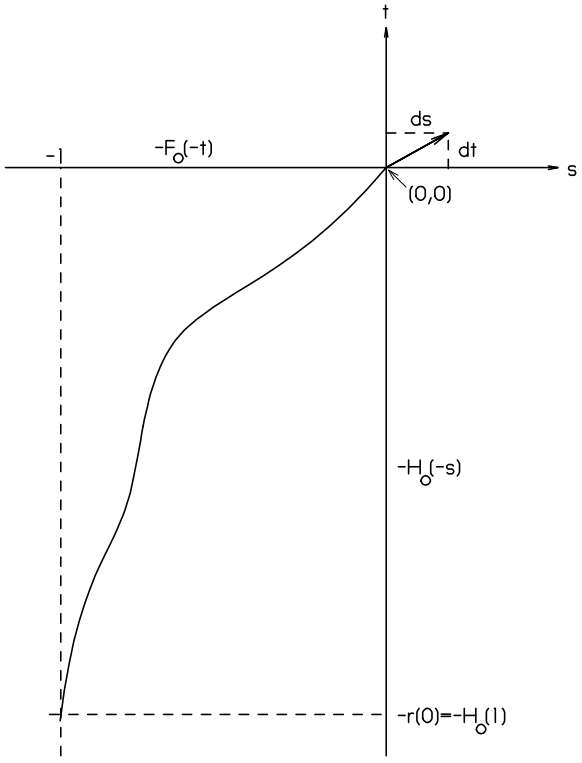

Figure 4: t over s

In the third quadrant,

$$t(s) = -H_0(-s) \qquad \text{for } -1 \le s \le 0 \tag{4}$$

(we take s as 0 at $t = 0$.) For $s \ge 0$ it is given by the differential equation (1), except that it depends of previous values of s through the current cutting age r. From Figure 4 we see that $r(t(s)) = t(s) - t(s-1)$, and substituting in (1),

$$\frac{\mathrm{d}t}{\mathrm{d}s} = \frac{1}{v} g[t(s) - t(s-1)] \qquad \text{for } s \ge 0\ . \tag{5}$$

This is a delay differential equation (DDE) with a constant (unit) delay. Given the initial age distribution and the harvesting rate, it uniquely determines t as a function of s. The distribution for any future time can be recovered from

$$H_{t(s)}(p) = t(s) - t(s-p) \; . \tag{6}$$

The quantity s is the cumulative harvested area. When $s = 1$ all the original forest has just been harvested and a new cycle commences, so that s can be interpreted as measuring "rotation units". The elapsed time $t(s)$ given by the DDE above reflects the changing rotation length.

We note a somewhat subtle point that can cause trouble later if ignored. For $s = 0$ the derivative $\frac{1}{v}g[H_0(1)]$ given by (5) is actually the *right derivative*, and may differ from the left derivative $H_0'(0)$ obtained from (4). In what follows, derivatives will be understood as right derivatives wherever the distinction is necessary. It is seen, however, that $t(s)$ is continuously differentiable for $s > 0$ (given that H_0 is continuous), with both the left and right derivatives coinciding with (5). Therefore, the distribution must satisfy

$$H_t'(0) = \frac{1}{v} g[H_t(1)] \qquad \text{for } t > 0 \; . \tag{7}$$

3.3 Related DDE's

Other DDE forms, possibly more widely studied or easier to handle, can be produced by change of variables.

Consider the cutting age as a function of s:

$$r[t(s)] \equiv y(s) = t(s) - t(s-1) \; . \tag{8}$$

Then, from (5),

$$\frac{\mathrm{d}y}{\mathrm{d}s} = \begin{cases} \frac{1}{v}g[y(s)] - \frac{1}{v}g[y(s-1)] & \text{if } s \geq 1 \\ \\ \frac{1}{v}g[y(s)] - H_0'(1-s) & \text{if } 0 \leq s < 1 \end{cases}$$

or

$$\frac{\mathrm{d}y}{\mathrm{d}s} = \frac{1}{v}g[y(s)] - \frac{1}{v}g[y(s-1)] \; ; \qquad s \geq 0 \; . \tag{9}$$

with

$$y(s) = g^{-1}[vH_0'(-s)] \qquad \text{for } -1 \leq s < 0 \; , \tag{10}$$

assuming g and H_0 continuous.

A third DDE, linear in the finite differences, is obtained defining

$$z(s) \equiv \frac{\mathrm{d}t}{\mathrm{d}s} = \frac{1}{v} g(y) \ . \tag{11}$$

Then,

$$\frac{\mathrm{d}z}{\mathrm{d}s} = \frac{1}{v} g'[g^{-1}(vz)][z(s) - z(s-1)] \ ; \qquad s \geq 0 \ , \tag{12}$$

with

$$z(s) = H_0'(-s) \qquad \text{for } -1 \leq s < 0 \ . \tag{13}$$

Remark: $g'[g^{-1}(u)] = 1/(g^{-1})'(u)$.

In terms of the forest regulation problem, $y(s) = r(t)$ is the cutting or oldest age after s rotations, and the duration of the rotation that ends at s. In forestry, the cutting age is commonly called *rotation*, probably by analogy to the normal forest situation. To avoid confusion I shall say "rotation s", use the plural, or call it *rotation number*, and shall refer to $y(s)$ as the cutting age or *rotation length*.

$z(s)$ is the ratio of harvestable volume per unit area to volume harvesting rate, or the reciprocal of the area harvesting rate. $vz(s)$ is the current yield, i. e. the volume per unit area for the cutting age of rotation s.

From (6) it is seen that there is a one-to-one relationship between the y and z functions and the evolution of the age distribution with s

$$H'_{t(s)}(p) = t'(s-p) = z(s-p) = \frac{1}{v} g[y(s-p)] \tag{14}$$

(assuming H_t and g continuous), generalizing (7), (10) and (13).

3.4 Integral equations

Instead of a DDE, we can state an integral equation for $y(s)$:

$$y(s) = t(s) - t(s-1) = \int_{s-1}^{s} dt(u) \ ,$$

and, using (1),

$$y(s) = \int_{s-1}^{s} \frac{1}{v} g[y(u)] \, \mathrm{d}u \ ; \qquad s \geq 0 \ , \tag{15}$$

defining $y(s)$ for $-1 \leq s < 0$ as in (10). This can also be obtained from (9). According to Baker (1996, see his equations (3.1) and (3.7)), it is a *Volterra integral equation of the second kind*, and more specifically a *convolution equation*[2]. The equivalent form

$$y(s) = \frac{1}{v} \int_0^1 g[y(s-u)]\,\mathrm{d}u$$

might on occasion be more convenient.

For $z(s)$, from (11),

$$z(s) = \frac{1}{v} g[\int_{s-1}^{s} z(u)\,\mathrm{d}u]\ ; \qquad s \geq 0\ , \tag{16}$$

or

$$z(s) = \frac{1}{v} g[\int_0^1 z(s-u)\,\mathrm{d}u]\ ,$$

with (13) for $s < 0$.

The interpretations are interesting. Equation (15) says that the average volume harvesting rate for any rotation, $(\int_{s-1}^{s} g[y(u)]\,\mathrm{d}u)/y(s)$, must equal v. This effectively ensures that the harvesting rate will be constant. Equation (16) shows that the slope of the curve of t over s at any point is a function (g/v) of the average slope over the previous unit s-interval. In this light, note the close correspondence between (16) and (5). Fluctuations are smoothed-out provided that g/v is not "too steep".

3.5 The method of steps

The DDEs described above can be transformed into a sequence of ordinary differential equations (ODEs) by the *method of steps* (Baker et al., 1995, for example). In this instance the process can be clearly explained introducing some new notation for function segments.

For y, for example, define $y_k(s) = y(k+s)$, where k is an integer and $0 \leq s < 1$. This corresponds to a segment of y with domain $[k, k+1)$. Conversely, with $k = [s]$ (i. e. the integer part of s), any $y(s)$ equals $y_k(s-k)$ in the segment that contains s. Then, substituting in (9),

$$\frac{\mathrm{d}y_k}{\mathrm{d}s} = \frac{1}{v} g(y_k) - \frac{1}{v} g(y_{k-1})\ ; \quad 0 \leq s < 1\ ; \quad k = 0, 1, 2, \ldots \tag{17}$$

[2]For other authors Volterra equations are linear (James, 1992; Petrovski, 1971).

For $k = 0$,

$$\frac{\mathrm{d}y_0}{\mathrm{d}s} = \frac{1}{v}g(y_0) - \frac{1}{v}g(y_{-1}) = \frac{1}{v}g(y_0) - H_0'(1-s) \ .$$

This is an ODE which, with the initial condition $y_0(0) = y(0) = H_0(1)$, uniquely determines $y_0(s)$ for $0 \le s \le 1$ (numerical integration would generally be required in practice.) Now, knowing $y_0(s)$, (17) for $k = 1$ is also an ODE, which with the initial condition $y_1(0) = y_0(1)$ determines the next segment $y_1(s)$. The argument is repeated for $k = 2, 3, \ldots$

The initial age distribution determines the oldest or cutting ages $y_0(s)$ during the first rotation, where $0 \le s \le 1$ is the elapsed fraction of that rotation (the harvested fraction of the initial forest.) Then, the cutting ages $y_1(s)$ for the second rotation are obtained from the known cutting ages $y_0(s)$ from the previous rotation, and so on.

Similar sequences of ODEs are obtained for t and z:

$$\frac{\mathrm{d}t_k}{\mathrm{d}s} = \frac{1}{v}g(t_k - t_{k-1}) \ ; \quad 0 \le s < 1 \ ; \quad k = 0, 1, 2, \ldots \tag{18}$$

$$\frac{\mathrm{d}z_k}{\mathrm{d}s} = \frac{1}{v}g'[g^{-1}(vz_k)](z_k - z_{k-1}) \ ; \quad 0 \le s < 1 \ ; \quad k = 0, 1, 2, \ldots \tag{19}$$

Note also that taking $s = k$ integer in (14) and (6), the relationships between the various characterizations of rotation k are

$$H'_{t(k)}(p) = z_{k-1}(1-p) = \frac{1}{v}g[y_{k-1}(1-p)] \tag{20}$$

$$H_{t(k)}(p) = t_{k-1}(1) - t_{k-1}(1-p) \ . \tag{21}$$

In terms of segments, the integral equations (15) and (16) just produce other integral equations:

$$y_k(s) = \int_0^s \frac{1}{v}g[y_k(u)]\,\mathrm{d}u + \int_s^1 \frac{1}{v}g[y_{k-1}(u)]\,\mathrm{d}u) \ ,$$

and

$$z_k(s) = \frac{1}{v}g[\int_0^s z_k(u)\,\mathrm{d}u + \int_s^1 z_{k-1}(u)\,\mathrm{d}u] \ ,$$

respectively.

4 Properties

As usual, existence and uniqueness questions are of more mathematical than practical interest. A properly formulated model should "make sense". Either way, formal proofs are straightforward, using for example the method of steps and standard ODE results.

4.1 No cycle limits

The asymptotic behavior of (9) and (15) is studied by Bélair (1991), in a more general situation where the time delay is a function of $y(s)$. He also presents results of Cooke and Yorke (1973) for a constant time lag. His *Theorem 3*, from Cooke and Yorke (1973), says that if g is continuously differentiable then, as $s \to \infty$, for every solution of (15) $y(s)$ tends to a constant or to $\pm\infty$. Actually, Bélair points out that differentiability of g is not necessary for this, a weaker local Lipschitz property suffices. This result effectively rules out the possibility of asymptotically oscillating solutions, as mentioned before.

4.2 Equilibria

It is clear, from (8) or (15) for example, that y cannot become negative (see also *Theorem 4* in Bélair (1991).) In addition, it does not matter in practice to assume that g has some (arbitrarily high) upper bound, and then the solutions of (15) cannot become unbounded. Therefore, if a forest does not become exhausted under an even volume harvest ($y(s) \to 0$), it must converge toward a normal forest with some constant finite cutting age r.

To find the possible stationary solutions we substitute $y(s) = r$ in (15):

$$r = \int_{s-1}^{s} \frac{1}{v} g[r] \, \mathrm{d}u = \frac{1}{v} g[r] \ ,$$

and any equilibrium cutting age ($\neq 0$) must therefore satisfy

$$g(r)/r = v \ , \tag{22}$$

as already "known" (Figure 1.) In other words, the MAI of the normal forest rotation equals the volume harvesting rate[3].

4.3 Potential pitfalls

The same result is obtained by substituting $z(s) = r$ or $t(s) = rs + c$ in (16) or (5), respectively. Substituting constants in (9) or (12), however, appears at first sight to indicate that any constant is a possible solution.

A similar situation is mentioned by Bélair (1991). He discusses a population model, in his notation,

$$x(t) = \int_{t-L[x(t)]}^{t} b(x(s))\,\mathrm{d}s\ , \tag{23}$$

where $L[x(t)]$ is a state-dependent time lag. This is equivalent to our equation (15) for a constant lag $L = 1$. Quoting in full (changing the equation numbers to agree with those here):

> "Differentiating both sides leads to the functional differential equation
>
> $$x'(t) = \frac{b(x(t)) - b(x(t - L[x(t)]))}{1 - L'[x(t)]b(x(t - L[x(t)]))} \tag{24}$$
>
> Although there is a close correspondence between solutions of (23) and (24), caution must be employed in using one equation to investigate the other (see Busenberg & Cooke, 1980), especially when numerical simulations are performed. For example, any constant $x(t) = \mathbf{x}$ is a solution of (24), whereas (23) only has, for stationary solutions, those constants that satisfy $\mathbf{x} = b(\mathbf{x})L(\mathbf{x})$. Also, the initial condition appropriate for a correct biological interpretation of (24) as a population model is not arbitrary but is incorporated in the integral form, (23). We analyze (23) and (24) together, considering that (24) is, literally, derived from (23)."

[3]Incidentally, with g unbounded it is seen in Figure 1 that $y(s) \to \infty$ can occur if v is small enough for the line $y = vs$ to remain always below the curve $y = g(s)$ without intersecting it.

Clearly (24) with $L = 1$ is equivalent to (9), and the analogy is obvious. What happens here is that not all solutions of the DDE are admissible. For a distribution uniform between 0 and r, $H_0(p) = r$, so that (10) implies condition (22). But with (12)-(13), if we ignore (11), the constraint has effectively been "lost" in the derivation.

However, (9) and (12) are still useful as *sufficient*, although *not necessary* conditions on the solutions. Especially given that these DDEs appear to have been investigated more than the integral equation alternatives.

4.4 Stability

If the forest can sustain a cut v, typically there will be two equilibrium or fixed points $y(s) = z(s) = r$ with r satisfying (22), points A and B in Figure 1 (in addition to $r = 0$.) What happens if there is a small perturbation in those steady-state solutions? For instance, if for a short time the cut differs from v, or the yield deviates from the expected? Then, after removing the perturbation, y and z may converge again toward r (the solution is *asymptotically stable*), or they may diverge, eventually settling at a different equilibrium point (the original solution was *unstable*.) In practice an unstable equilibrium would never be reached.

More precisely, the relevant definitions are as follows (for example Baker et al., 1995; Baker, 1996). An equilibrium solution r is *stable* if, for any $\epsilon > 0$, there is a δ such that if the initial data of another solution is within a distance δ from r then all future values will not differ from r by more than ϵ. That is, if $y(u)$ is any solution such that $|y(u) - r| \leq \delta$ for $s - 1 \leq u \leq s$, then $|y(u) - r| \leq \epsilon$ for all $u > s$. The solution r is *asymptotically stable* if, in addition to being stable, any other solution initially within a small enough δ converges to r: $|y(u) - r| \leq \delta$ for $s - 1 \leq u \leq s$ implies $|y(u) - r| \to 0$ as $u \to \infty$. A solution is *unstable* if it is not stable.

The usual approach to stability of DDEs is based on local linearization. Thus, the linearization of (9) around r is

$$\frac{\mathrm{d}y}{\mathrm{d}s} = \frac{1}{v} g'(r)[y(s) - y(s-1)] \, .$$

The condition for stability of this linear DDE is $g'(r) < v$ (Bélair, 1991, page 174). We would conclude then that B in Figure 1 would be stable and A unstable, as had been conjectured before (Section 2.) C would also be

unstable, as might be expected (but see Section 5.5.) Because the only equilibrium solutions correspond to those points, stability has to be asymptotic.

Two aspects of this analysis, however, appear unsatisfactory. First, it is not clear to me to what extent the linearization is valid in this case. That is, if this *stability in variation* or *stability in first approximation* (Baker et al., 1995) implies stability of the non-linear DDE as defined above. Second, it is clear from (9) that, regardless of $g'(r)$, any constant perturbation $r+\delta$ would remain unchanged (also true for the linearized equation), contradicting the conclusions. Obviously, there are complications arising from the fact that not all perturbations are "admissible", as explained in Section 4.3[4].

It seems possible to carry out a much more direct stability analysis, avoiding the problems of linearization and of inadmissible solutions. Consider equation (16), and let r be an equilibrium point, a zero of (22). For any solution $z(s)$ of (16),

$$\begin{aligned} \sup_{s-1<u<s} |z(u) - r| \leq \delta \quad &\Rightarrow \quad |\int_{s-1}^{s} z(u)\,\mathrm{d}u \; - \; r| \leq \delta \\ &\Rightarrow \quad \frac{1}{v} g(r-\delta) \leq z(s) \leq \frac{1}{v} g(r+\delta) \;, \end{aligned}$$

with $\delta > 0$. If $g'(r) < v$ then $g(y)$ has a downward crossing of the line vy at $y = r$. Therefore, $g(r+\delta) < v(r+\delta)$, at least for δ not too large. Similarly, $g(r-\delta) > v(r-\delta)$. It follows that for δ small enough $z(s) - r$ is strictly bounded by $\pm\delta$. The same argument ensures that the bound remains valid for larger values of s (and in fact decreases with s.)

We conclude that if $g'(r) < v$ at an equilibrium point r, then r is asymptotically stable[5]. A proof of instability if $g'(r) \geq v$ could possibly be obtained along similar lines, but I have not worked out the details.

4.5 Basins of attraction

The really interesting question is to distinguish those age distributions that converge to a stationary solution from those that diverge to zero. That is, to find the basins of attraction of zero and of the stable fixed point. Unfortunately there are no significant advances in this direction yet.

[4] I am indebted to Brian Hassard for useful discussion on this issue

[5] Note that the requirement of differentiability of g can be easily relaxed.

We might speculate that the unstable fixed point (r such that $g(r) = vr$ and $g'(r) > v$) could play a role in delimiting those domains. Perhaps if some appropriate invariant functional could be found, a real-valued transformation of the age distribution that remained constant over time, its value for the unstable equilibrium normal forest could separate the sustainable and unsustainable distribution classes (see also Section 6.3.)

5 Discrete models

The continuous model discussed up to here seems convenient for obtaining analytical results and insights. For simulation and numerical results, however, it is necessary to use discrete formulations. These may be based on close approximations to the continuous case, as when using numeric integration techniques, or may be discrete models derived by direct reasoning about the practical problem.

5.1 The classical forest regulation model

The classical approach partitions the forest into equal-width age classes, and looks at the process as advancing by discrete time steps. The time steps are equal to the age class width. In the simplest situation there is only one kind of forest stand, characterized by one yield table that assigns a fixed volume per unit area to each class. To be specific, let us assume one-year steps and classes. Then, for the simple problem that we have been considering the evolution of the system can be described as follows.

For any year t, the state of the forest is given by the areas in each age class, a vector $\mathbf{a}_t \equiv (a_{t1}, a_{t2}, \ldots, a_{tm})$. Let the areas cut from each class be $\mathbf{c}_t \equiv (c_{t1}, c_{t2}, \ldots, c_{tm})$. Then, assuming that the areas cut are replanted immediately, the state in year $t+1$ is obtained by subtracting $\mathbf{c}_t$ from $\mathbf{a}_t$, shifting forward by one age class, and making the new first age class equal to the total area cut:

$$\begin{aligned} a_{t+1,i+1} &= a_{ti} - c_{ti} \; ; \qquad i = 1, \ldots, m \\ a_{t+1,1} &= \sum_i c_{ti} = A - \sum_{i>1} a_{t+1,i} \; , \end{aligned}$$

where A is the total area. The number of classes m is dynamically made as large as necessary or, alternatively, class m is taken as open (i. e., it

represents ages $\geq m$) and any areas that would shift to $m+1$ accumulate there.

The volume cut is $v_t = \mathbf{g}\mathbf{c}_t$, where $\mathbf{g} \equiv (g_1, g_2, \ldots, g_m)$ is the yield table. In this model it is obtained by cutting oldest ages first, making $c_{ti} = a_{ti}$ as necessary for $i = m, m-1, \ldots$ until the required v_t is completed, in general cutting only a fraction of the final remaining class[6].

It is clear that an initial age distribution and a given constant volume cut $v_t = v$ completely determine the evolution of the system. It may converge to a uniform distribution (except possibly for the oldest age class), or it may reach a point where it is not possible to continue harvesting v. The implementation of simulations is straightforward. Analysis is somewhat complicated by the volume cut accumulation procedure, and by the fractional oldest non-empty age class. The model is related to the continuous formulation of equation (2). We return to this in Section 6.3.

5.2 A different discretization

The classical model groups forest stands of increasing age into fixed age classes with variable areas. Consider instead grouping into fixed area classes with variable ages. In addition, use variable time steps, so that a whole class is cut in each step. The total area A is distributed into n equal-area classes which at step k have ages $x_{k1} \leq x_{k2} \leq \cdots \leq x_{kn}$. In other words, instead of describing the forest by the age histogram we use n quantiles from the distribution, $\mathbf{x}_k \equiv (x_{k1}, x_{k2}, \ldots, x_{kn})$ [7]. There is a continuous yield function $g(x)$ and a constant annual volume cut v.

The state transitions are simple, just shift to the right and add the time step length:

$$\begin{aligned} x_{k+1,i+1} &= x_{ki} + \Delta t_k \; ; \qquad i = 1, \ldots, n-1 \\ x_{k+1,1} &= \Delta t_k \; . \end{aligned}$$

[6] It can be shown that under many circumstances this strategy is optimal (García, 1990)

[7] The exact interpretation of the x_{ki} may vary somewhat. They may be seen as quantiles of a continuous distribution, or as average or representative ages for each class. Or, more simply, the distribution may be thought as being discrete. In any case, in the calculations it is assumed that all the area in a class has the same age. The problem of choosing representative quantiles is related to the selection of "plotting positions" in nonparametric statistics; one could also shift slightly the yield function to adjust for bias due to the quantiles location.

The step length $\Delta t_k = t_{k+1} - t_k$ is the time it takes to harvest the last class, which contains A/n units of area of age x_{kn}:

$$\Delta t_k = \frac{Ag(x_{kn})}{nv} \ .$$

As before, in what follows I shall drop the constant A by assuming that $A = 1$, or by expressing v on a per unit area basis.

An advantage of this formulation, from a simulation point of view, is maintaining at all times a consistent level of resolution in the forest representation, with a fixed size array. As in the classical approach the shifts may be avoided by keeping a pointer into the array. In pseudocode the basic algorithm could be as follows:

Initialize:

read $\mathbf{x}$

$k, t \leftarrow 0$

Loop:

$p \leftarrow 1 + (k-1)_{(\mathrm{mod}\ n)}$

$\Delta t \leftarrow \frac{1}{nv} g(x_p)$

$x_p \leftarrow 0$

$\mathbf{x} \leftarrow \mathbf{x} + \Delta t$

$k \leftarrow k + 1$

$t \leftarrow t + \Delta t$

output $k, t, \mathbf{x}$

Here n steps make one "rotation", that is, the whole area is recycled every n steps. Therefore, it may be of interest to compute also the elapsed "rotation units", $s_k = k/n$.

5.3 Simplifications and analogies

Further streamlining of the computations is possible, leading to discrete analogs of the DDEs and integral equations discussed before.

First, note that oldest age is

$$x_{kn} \equiv y_k = t_k - t_{k-n} \ ,$$

if we define $t_{-u} = -x_{0u}$ for $u = 1, \ldots, n$. Then, it is sufficient to keep track of t,

$$t_{k+1} = t_k + \Delta t_k \ ,$$

where

$$\Delta t_k = \frac{1}{nv} g(t_k - t_{k-n}) \ . \tag{25}$$

This is analogous to (5). A closer analogy may be written as

$$\frac{\Delta t_k}{\Delta s_k} = \frac{1}{v} g(t_k - t_{k-n}) \ ,$$

noting that $\Delta s_k \equiv s_{k+1} - s_k = 1/n$.

If needed, any x_{ki} could be recovered from

$$x_{ki} = t_k - t_{k-i} \ .$$

For testing sustainability, though, t is sufficient. If the "instantaneous rotation length" $z_k \equiv \Delta t_k / \Delta s_k = n \Delta t_k$ tends to a positive constant, then that is the equilibrium normal forest rotation, and the cutting rate v is sustained. If z_k tends to zero it means that v is not sustainable. The reciprocal of z might be interpreted also as a measure of cutting intensity.

The simulation algorithm becomes:

Initialize:

$$\begin{aligned} \text{read} \quad & \mathbf{x} \\ \mathbf{t} \quad & \leftarrow \quad -\mathbf{x} \\ k, t \quad & \leftarrow \quad 0 \end{aligned}$$

Loop:

$$\begin{aligned} p \quad & \leftarrow \quad n - k_{(\text{mod } n)} \\ y \quad & \leftarrow \quad t - t_p \\ z \quad & \leftarrow \quad \frac{1}{v} g(y) \\ \text{output} \quad & \quad k, t, k/n, y, z \\ t_p \quad & \leftarrow \quad t \\ t \quad & \leftarrow \quad t + z/n \\ k \quad & \leftarrow \quad k + 1 \end{aligned}$$

Alternatively, we could keep track of the cutting age y_k. We have

$$y_k = t_k - t_{k-n} = \sum_{k-n}^{k-1} \Delta t_i \ ,$$

from where,

$$y_k = \sum_{k-n}^{k-1} \frac{1}{nv} g(y_i) \ , \tag{26}$$

the analog of (15). Maintaining a record of the last n values of y this may be used directly to calculate the next y. Or y may be updated as $y_{k+1} = y_k + \Delta y_k$, where the formula for the increment, similar to (9), results from differencing the previous expression:

$$\Delta y_k = y_{k+1} - y_k$$

$$\Delta y_k = \frac{1}{nv} g(y_k) - \frac{1}{nv} g(y_{k-n}) \ . \tag{27}$$

The necessary initial values y_k for $k < 0$ are a bit messy. It is found that they must be $y_{-1} = g^{-1}[nvx_{01}]$, and $y_{-i} = g^{-1}[nv(x_{0i} - x_{0,i-1})]$ for $1 < i \leq n$.

A third possibility is to work with the quantities $z_k = n\Delta t_k = g(y_k)/v$. The discrete analog of (16) is

$$z_k = n\Delta t_k = \frac{1}{v} g(t_k - t_{k-n}) = \frac{1}{v} g(\sum_{k-n}^{k-1} \Delta t_k)$$

$$z_k = \frac{1}{v} g(\frac{1}{n} \sum_{k-n}^{k-1} z_i) \ , \tag{28}$$

with $z_{-1} = nx_{01}$, and $z_{-i} = n(x_{0i} - x_{0,i-1})$ for $1 < i \leq n$. No convenient difference equation similar to (12) is found, however.

All these formulas require more calculation. A mixed strategy is quite efficient, though. We update y keeping a history of z:

$$\begin{aligned} z_k &= \frac{1}{v} g(y_k) \\ y_{k+1} &= y_k + (z_k - z_{k-n})/n \ . \end{aligned}$$

It works like this:

$$
\begin{array}{rcl}
\text{Initialize:} & & \\
\quad \text{read} & \mathbf{x} & \\
\quad y & \leftarrow & x_n \\
\quad z_1 & \leftarrow & n x_1 \\
\quad z_i & \leftarrow & n(x_i - x_{i-1}) \; ; \quad i = 2, \ldots, n \\
\quad k, t & \leftarrow & 0 \\
\text{Loop:} & & \\
\quad z & \leftarrow & \dfrac{1}{v} g(y) \\
\quad p & \leftarrow & n - k_{(\mathrm{mod}\ n)} \\
\quad y & \leftarrow & y + (z - z_p)/n \\
\quad \text{output} & & k, t, k/n, y, z \\
\quad z_p & \leftarrow & z \\
\quad t & \leftarrow & t + z/n \\
\quad k & \leftarrow & k + 1
\end{array}
$$

Actually, there is little to choose between this and the algorithm that uses the $\mathbf{t}$ vector.

5.4 Numerical integration

Instead of formulating directly the problem as an approximation in discrete time, one might use a continuous model and discretize it in order to compute an approximate numerical solution. Although in fact it is somewhat debatable which model, discrete or continuous, represents reality more accurately. Trees often have a relatively short annual growing season, and cuts occur at discrete points in time.

In general, the numerical integration of delay differential equations can be very complex (Baker et al., 1995; Baker, 1996). It is easier in the present situation, though, where the delay is constant and the solutions are continuous and smooth (except possibly at time zero.)

The *method of steps* shows most clearly the connection with ordinary differential equations. As shown in Section 3.5, the problem reduces to integrating a sequence of ODEs over successive rotation segments. Computing

the solution over a segment makes use of the solution over the previous segment. The only complication is that, with the usual variable time-step integration methods, it is not possible to predict the points for which the previous segment solution will be needed. It is necessary then to have some "dense-output" facility to interpolate non-meshpoint solution values, and sophisticated strategies for doing this are possible (Baker et al., 1995).

A constant s-step size $h = 1/n$ for some integer n greatly simplifies the problem, at the cost of additional computing expense and/or reduced accuracy. The solution is computed at each point $s_k = kh$, knowing the values at the previous n points. Euler's method applied to (5) gives

$$t(s_k + h) = t(s_k) + \frac{h}{v} g[t(s_k) - t(s_k - 1)]$$

or

$$t(s_{k+1}) = t(s_k) + \frac{1}{nv} g[t(s_k) - t(s_{k-n})] \ ,$$

which is the same as (25). Similarly, Euler integration of (9) gives (27). Therefore, the discrete model of Sections 5.2 and 5.3 may be seen as a numerical solution to the continuous model.

It is well-known that Euler's method is not very reliable, although it is probably adequate with a large enough n. More sophisticated ODE numerical integration methods could be used, but it seems simpler to work with the integral equation forms instead. With the same step length as before, (15) may be approximated by a numerical quadrature of the form

$$y(s_k) \equiv y_k = \frac{1}{v} \sum_{i=1}^{n} w_i g(y_{k-1}) = \sum_{i=1}^{n} w_i z_{k-1} \ . \tag{29}$$

Equal weights $w_i = 1/n$ (the rectangular integration rule) result in (26). Again an equivalence with the discrete model, and the simplifications of Section 5.3 are applicable. More accurate alternatives could be easily used directly with (29), e. g., a modified Simpson's rule or a semi-open[8] Newton-Cotes formula. Although unlikely to make much difference in practice, other quadrature refinements come to mind: methods based on Fourier instead of polynomial approximations, use of more than n previous values[9], use of previous values of both y and z (which links with ODE integration methods such as Adams-Bashforth, see Chapter 13 in Hamming, 1962).

[8] Function values are available for one of the two ends of the integration interval. (See also the footnote in Section 5.2.)

[9] A connection between the DDE solution and an analytical continuation of the initial segment?

5.5 Examples

The first algorithm of Section 5.3 has been programmed in APL (Appendix 1). The examples use the yield function $g(y) = \exp(1 - 1/y)$ shown in Figure 1. To make things easier, the scaling in this function is such that the maximum mean annual increment is 1 at age 1 [10].

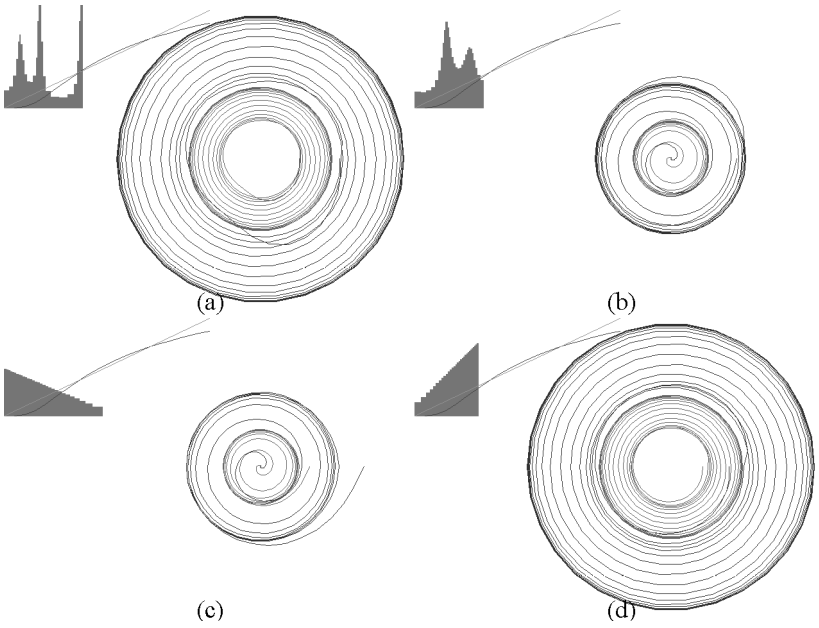

Figure 5: Four simulations, $v = 0.95$

Output is shown graphically on screen as the simulation progresses (Figure 5). The values of y and z are plotted in polar coordinates, with an angular step of $2\pi/n$ radians. Thus, appropriately enough, one full turn represents one rotation. The red outside spiral is z, and the green inside one, at half the scale, is the cutting age y. These examples used $n = 30$. For reference, the initial age distribution, the yield curve and the vy line are displayed on the upper left. Actually, the distribution is discrete, with equal areas at each of the points in the supplied ages list, but a histogram approximation

[10] In real life one of these age/time units would typically be 20 to 200 years, depending on tree species and site productivity. One yield unit might be of the order of 1000 cubic meters per hectare.

is shown to facilitate visualization[11].

In Figure 5 $v = 0.95$, that is, the cut is 95 % of the maximum MAI. Depending on the initial age distribution, the constant cut v is or is not sustainable. Always y and z either converge to the stable equilibrium (point B in Figure 1), or they crash to zero in a "death spiral". Changing the scale of the initial distribution shows that the transition between both cases occurs when the oldest age is close to the unstable fixed point (A in Figure 1.) The exact position, however, depends of the distribution shape. All these instances are close to that critical situation. Under those conditions it is observed that convergence to the equilibrium normal forest can be very slow, while forest exhaustion is usually faster.

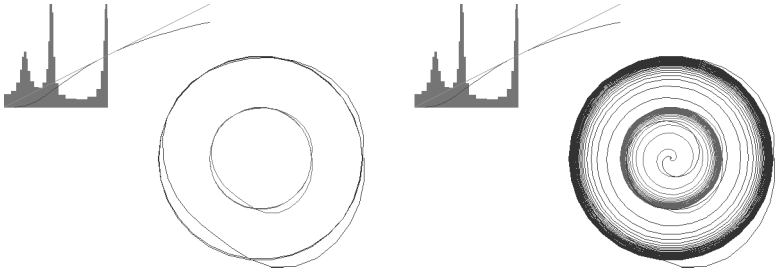

Figure 6: A simulation with $v = 1$: (a) after 130 rotations, (b) after 170 rotations.

The dynamics when the cut equals the maximum MAI, $v = 1$ here, is interesting. Theoretically the equilibrium point (C in Figure 1) is unstable. However, often the simulation initially seems to converge to the equilibrium, with the graph remaining unchanged for a long time before finally collapsing (Figure 6.) The fixed point appears as an attractor for distributions coming from "above", repelling those "below", a sort of saddle point. Presumably, the observed final collapse is caused by small perturbations due to round-off error. For all practical purposes, though, a maximum MAI cut can be sustainable, especially considering that slight feedback corrections by the manager can stabilize the system.

[11]The variable class width histogram is computed from a polygonal cumulative distribution function passing through the origin and through the points $(x_{0i}, i/n)$, $i = 1, \ldots, n$.

6 Dynamics in $\Re^2$

Discrete models with 2 or 3 classes are obviously quite inadequate for practical use. However, for $m = 3$ and $n = 2$ the properties of the models of Section 5 are easily visualized graphically, and some important points become particularly clear in this the simplest of situations. Perhaps surprisingly, analytical solutions are still far from trivial. Solving these simpler problems would be a crucial first step, and they are also a source of ideas and insight for the study of the functional differential equations

6.1 States and transitions

The behavior of a dynamic system is conveniently specified by a state vector, that describes current conditions, and a transition function, that determines the changes of state (e. g., Padulo & Arbib, 1974). The various state descriptions and transition functions already seen in sections 5.2 and 5.3 are summarized here for $n = 2$. The extension to any n is straightforward, but the essential points are seen more clearly in these specific instances.

Using the age list, the state of the forest is characterized by the x_{ki} and the current time t_k, a three-dimensional state vector. The state is updated by the transition function

$$\begin{aligned} x_{k+1,1} &= f(x_{k2}) \\ x_{k+1,2} &= x_{k1} + f(x_{k2}) \\ t_{k+1} &= t_k + f(x_{k2}) \end{aligned} \tag{30}$$

writing $g(x)/(nv) \equiv f(x)$. For investigating asymptotic behavior, for example, we may not be interested in the correspondence between the stage numbers k and the actual times t_k, so that a two-dimensional state space may be sufficient.

Instead of this, three consecutive time values make an equivalent state vector $(u_{k1}, u_{k2}, u_{k3}) \equiv (t_{k-2}, t_{k-1}, t_k)$. From (25),

$$\begin{aligned} u_{k+1,1} &= u_{k2} \\ u_{k+1,2} &= u_{k3} \\ u_{k+1,3} &= u_{k3} + f(u_{k3} - u_{k1}) \end{aligned} \tag{31}$$

The reduction to two dimensions is not possible here.

With (26), a state vector is $(u_{k1}, u_{k2}, u_{k3}) \equiv (y_{k-1}, y_k, t_k)$, and

$$\begin{aligned} u_{k+1,1} &= u_{k2} \\ u_{k+1,2} &= f(u_{k1}) + f(u_{k2}) \\ u_{k+1,3} &= u_{k3} + f(u_{k2}) \end{aligned} \tag{32}$$

Again, we may ignore the third component.

In contrast, the difference equation (27) is

$$y_{k+1} = y_k + f(y_k) - f(y_{k-2}) \ ,$$

and attempting to use this would require keeping a record of three values of y instead of two. The presence of a redundant state variable in this formulation reaffirms our previous observations that equations (15) and (26) are somehow "more fundamental" than (9) and (27).

Finally, (16) gives the state vector $(u_{k1}, u_{k2}, u_{k3}) \equiv (z_{k-1}, z_k, t_k)$, and the transition function

$$\begin{aligned} u_{k+1,1} &= u_{k2} \\ u_{k+1,2} &= h(u_{k1} + u_{k2}) \\ u_{k+1,3} &= u_{k3} + u_{k2}/2 \end{aligned} \tag{33}$$

with $h(x) \equiv g(x/2)/v$.

The dynamics of y and z may also be described by simple-looking second-order recurrence relationships:

$$y_k = f(y_{k-1}) + f(y_{k-2})$$

$$z_k = h(z_{k-1} + z_{k-2}) \ .$$

6.2 Basins of attraction

With (30), (32) or (33), the sets of initial values that lead to sustainability or to exhaustion can be shown graphically in the plane. For each graphics pixel representing an initial point (x_{01}, x_{02}) or (u_{01}, u_{02}), the first two transition equations are iterated until convergence to either $(0, 0)$ or to the stable normal forest is determined, and the pixel colored accordingly.

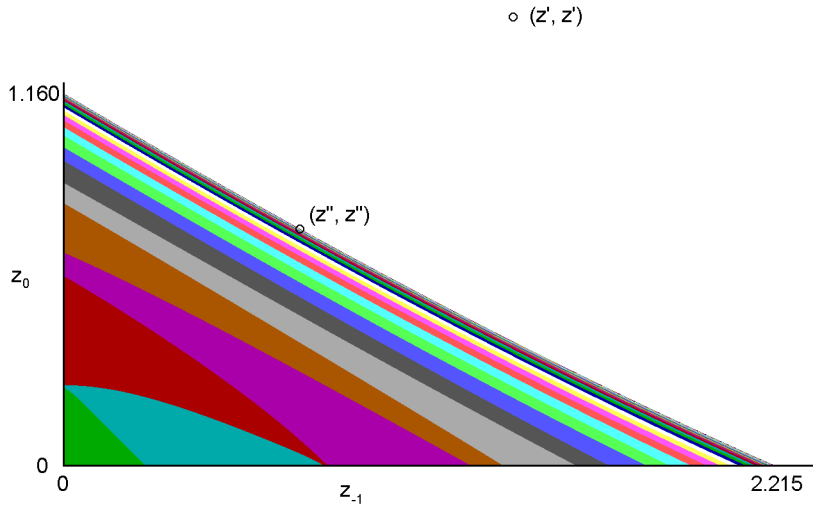

Figure 7: Unsustainable z values, $v = 0.95$ (see text)

Fractint, a public domain program normally used for producing fractals, was found to be a convenient tool for generating and exploring these graphs (Appendix 2). The simplest sets are obtained with (33). Figure 7 shows the result for $g(y) = \exp(1 - 1/y)$ with $v = 0.95$. The unsustainable set (the basin of attraction of $(0, 0)$) is shaded, with the gray levels corresponding to a color coding of the number of iterations performed. The white points in the rest of the first quadrant are sustainable, eventually converging to the stable equilibrium (z', z'), i.e., they constitute the basin of attraction of (z', z').

$z' \approx 1.40261$ is the stable fixed point, solution of $g(z)/v = h(2z) = z$. As might be expected, the boundary between the two basins of attraction passes through (z'', z''), where $z'' \approx 0.737810$ is the unstable fixed point. Zooming in with Fractint the boundary appears smooth, with a similar banding pattern at all scales and no indications of fractal structures or chaotic behavior.

It is seen that the corner near $(2.215, 0)$ is taken by the transition to the other corner, approximately $(0, 1.160)$. This, in turn, goes to a point on the boundary curve. Clearly, points on that curve remain on the curve, eventually approaching (z'', z'').

A very similar picture is obtained for the maximum MAI cut $v = 1$. There

the boundary passes through the fixed point $(1, 1)$, with corners near $(3.47, 0)$ and $(0, 1.53)$. Equations (30) and (32) also produce smooth boundaries, although more curved.

It is rather intriguing that it is not known how to directly calculate the apparently simple boundary curve of Figure 7.

6.3 The classic model with three age classes

For $m = 3$, the behavior of the "classic" model of Section 5.1 can also be displayed in the plane. The areas a_1 and a_2 may be used as coordinates, given that the total $a_1 + a_2 + a_3 = A$ must be constant. Or, for a more attractive presentation, isometric coordinates could be used.

Systematic simulation becomes somewhat complicated by the effect of different yield patterns, represented by two essential additional parameters apart from v. Limited experimentation with Fractint shows apparently linear basin of attraction boundaries (and parallel iteration bands.) An exhaustive algebraic analysis seems feasible, although tedious due to the various cases to be enumerated.

If the linearity is confirmed, we might conjecture that it extends to higher dimensions and to the continuous model. The desired discriminant functional for sustainability might then be of the form

$$Q = \int_0^\infty \varphi(x)\,\mathrm{d}F_t(x)$$

for some function $\varphi(x)$, using the notation of Section 3.1. From here,

$$Q = \int_0^1 \varphi[H_t(p)]\,\mathrm{d}p = \int_0^1 \varphi[t(s) - t(s-p)]\,\mathrm{d}p = \int_0^1 \varphi[\int_0^p z(s-u)\,\mathrm{d}u]\,\mathrm{d}p\ .$$

This would suggest that perhaps the equation of the curve in Figure 7 has the form

$$\varphi(z_{-1}) + \varphi(\frac{z_{-1} + z_0}{2}) = \text{constant}\ .$$

It is not at all clear how to find φ, though.

7 Discussion and conclusions

A sustainable forest harvesting model has been formulated in terms of delay differential equations and of nonlinear integral equations. Using this, previous conjectures about the location and stability of steady-state solutions have been formally proved. The less obvious possibility of limit cycles has been ruled out.

The main problem, determining the sustainability or not of a harvesting level for any given initial age distribution, remains an open question. However, linking the problem to an active and well-established mathematical discipline, the theory of functional differential equations, might attract the interest of mathematicians and contribute new tools for advancing toward a solution. Conversely, this model might help in the development of the theory as a testing ground for concepts and a source of ideas. I must admit that, apart from looking at Bellman and Cooke (1963) many years ago, I have not had the opportunity yet of studying the more recent texts on the subject: El'sgol'ts and Norkin (1973), Driver (1977), Hale (1977), Kolmanovskii and Myshkis (1992), Kuang (1993).

Discrete versions serve as a complement to the continuous functional differential equation models. They are convenient for simulation and experimentation. In addition, they provide mathematically simpler analogies that throw some light into issues that are rather subtle in the continuous setting. A particularly interesting instance is the ambiguity/redundancy in some DDEs noted by Busenberg and Cooke (1980) and Bélair (1991), and discussed in sections 4.3, 5.3 and 6.1.

Although unrealistic from a practical point of view, studying the behavior of low-dimensional discrete models was found useful to better understand the fundamentals. These "bare bones" models allow stating the crucial questions in the simplest possible setting. Even then, the key problem does not seem easy to solve. Essentially, it can be distilled into the following. Consider the recurrence

$$z_{k+2} = f(z_k + z_{k+1}) \ ,$$

where $f(x) = 3\exp(-2/x)$, for example, and $z_i \geq 0$. It is known that z_k will either converge to 0 or to $1.6153\ldots$. Which initial pairs (z_1, z_2) lead to 0? Answering this appears to be a necessary first step for further work.

Appendix 1. Simulation program

The examples in Section 5.5 used an *APL*PLUS* implementation of the first algorithm of Section 5.3. A free interpreter is found on the Internet at *ftp://watserv1.uwaterloo.ca/languages/apl/apl-plus/index.html*.

The main routine, or *function* in APL jargon, is

```
    ∇ key←v SIM X;T;n;k;t;p;y;z;last_point
[1]   Initialize
[2]   n←⍴T←-X
[3]   k←t←0
[4]  LOOP:
[5]   p←n-n|k
[6]   y←t-T[p]
[7]   z←(*1-÷y⌈1E¯3)÷v
[8]   Output(k÷n),y,z
[9]   T[p]←t
[10]  t←t+z÷n
[11]  k←k+1
[12]  →(0=⍴,key←⎕INKEY)/LOOP
[13]  Finish
    ∇
```

For clarity it follows closely the algorithm pseudocode, ignoring questions of APL conventional style or efficiency (in particular, avoiding the notorious APL "one-liners".) The function is called with the cutting level v as left argument, and a vector of (increasing) class ages on the right. It runs until interrupted by pressing any key, and returns that key for possible use by calling functions. As an example, entering `0.98 SIM +\(?30⍴100)÷1500` runs a simulation that starts with a random initial distribution.

The function `SIM` itself is standard APL, except for the key-press test on line 12. It calls three functions that use graphics and keyboard control functions peculiar to *APL*PLUS*. The first one computes the initial point on the curves, initializes graphics and keyboard (the `POKE` suppresses the `INKEY` default wait for a key-press), and draws the histogram and yield curve:

```
    ∇ Initialize;U
[1]   last_point←0,(¯1↑X),(*1-÷¯1↑X)÷v
[2]   ⎕MOUSE[1]←0
```

```
[3]   U←0 ⎕POKE 254 ⋄ U←⎕INKEY
[4]   U←8 ⎕GINIT 'IBMCOLOR'
[5]   U←⎕GWINDOW 0 0 4 3
[6]   3 ⎕GLINE(¯1↓0,X),1,X,[1.5]0⌈1-÷(4×⍴X)×X-¯1↓0,X
[7]   5 ⎕GLINE 1 20 2 ⍴U,[1.5]1-0.5×*1-÷U←0.1×⍳20
[8]   6 ⎕GLINE 1 2 2 ⍴ 0 1 2 ,1-v
    ∇
```

The second one draws the y and z spiral segments:

```
    ∇ Output SYZ;M
[1]   M←,⍉ 2 1 ∘.○(○2)×last_point[1],SYZ[1]
[2]   2 ⎕GLINE 1 2 2 ⍴ 2.5 1.5 2.5 1.5 +M×2/0.5×last_point[2],SYZ[2]
[3]   4 ⎕GLINE 1 2 2 ⍴ 2.5 1.5 2.5 1.5 +M×2/last_point[3],SYZ[3]
[4]   last_point←SYZ
    ∇
```

The final function just returns to text mode and resets *INKEY* to its default behavior:

```
    ∇ Finish;r
[1]   r←3 ⎕INT 16
[2]   r←1 ⎕POKE 254
    ∇
```

Appendix 2. Exploring low-dimensional dynamics with Fractint

Fractint is a computer program for the graphical manipulation and display of various types of fractals. Versions for several platforms are freely available, for instance on the Internet at *http://spanky.triumf.ca/www/fractint/fractint.html*

In addition to many built-in fractals, there is a "formula" feature for specifying other equations in a simple programming language. After familiarizing oneself with the most important of the myriad of options and commands, Fractint can thus become a convenient tool for studying the behavior of low-dimensional systems, fractal or not. The variety of calculation and display options, easy scale and parameter changes, and the ability to zoom into picture details at arbitrary depths are particularly useful.

The "formula" for producing Figure 7 was as follows:

```
Zforest{
        old=real(pixel), new=imag(pixel)
        v=real(p1)
        :
        temp = new
        new = exp(1-4/(new+old+0.01+abs(new+old-0.01)))/v
        old = temp
        z = old + flip(new)
        |z| > 0.000001
        }
```

Fractint works with complex arithmetic. For each pixel, it first performs the initialization code up to the colon. Here it reads the point previous and current z values, and obtains the cutting level supplied by the user in parameter `p1`. Then the instructions that follow are iterated until either the last statement becomes false, a specified maximum number of iterations is reached, or a recurring pattern in the special (complex) variable `z` is detected. By default, in the first instance the pixel is colored according to the number of iterations reached, and with a background color otherwise. A protection against overflow and division by zero has been included by taking the maximum between `old+new` and 0.01, although it did not seem to make any difference in practice.

The user must supply the v level, and appropriate upper-left and bottom-right corner coordinates for display. For some reason computations were much faster with the floating-point arithmetic option (`f` command or `x` menu) than with the fixed-point default. In case of doubt it is wise to check results by disabling the "guessing" calculation mode, increasing the iteration limit (both in the `x` menu), and disabling periodicity checking (`g` followed by `periodicity=no`). Coordinates may be read with the cursor in the *orbit* mode activated with `o n`.

The "classic" model with $m = 3$ may be implemented as follows

```
classic{
        a1=real(pixel), a2=imag(pixel), a3=1-a1-a2
        g1=real(p1), g2=imag(p1)
        v=real(p2)
        :
```

```
IF (a3 < 0)
    a2 = -1
ELSE
    if (v <= a3)
        a2 = a1
        a1 = v
        a3 = 1-a1-a2
     elseif (v <= a3+g2*a2)
         a2 = a1
         a1 = a3+(v-a3)/g2
         a3 = 1-a1-a2
     elseif (g1 > 0)
         a2 = a1-(v-a3-g2*a2)/g1
         a1 = 1-a2
         a3 = 0
     else
         a2 = -1
     endif
ENDIF
z = a1 + flip(a2)  ; for periodicity check
;
a2 > 0
}
```

The third age class is taken as open and, without loss of generality, it has been assumed that $A = g_3 = 1$. The user supplies v and the yields g_1, g_2 for age classes 1 and 2. The display coordinates are a_1 and a_2, and the proper corners $(0, 1)$, $(1, 0)$ must be specified (the outside `IF` forces the background color on the "impossible" $a_1 + a_2 > 1$ region.) Note that the *if-then-else* construct is only available in the latest PC version (19.6) of Fractint.

An isometric graph might be produced by substituting `a1 = (sqrt(3)* real(pixel) - imag(pixel))/2` for the first assignment. The triangle delimiting the relevant region would need to be added somehow to facilitate visualization.

References

Allison, B. J. (1978). *Some Aspects of Forest Planning.* NZ Forest Products, Tokoroa, New Zealand.

Baker, C. T. H., Paul, C. A. H., & Willé, D. R. (1995). Issues in the Numerical Solution of Evolutionary Delay Differential Equations. *Adv. Comp. Math.*, *3*, 171–196.

Baker, C. T. H. (1996). Numerical Analysis of Volterra Functional and Integral Equations — State of the Art. Numerical analysis report 292, Manchester Centre for Computational Mathematics, Department of Mathematics, The University of Manchester. Internet URLs: http://www.ma.man.ac.uk/MCCM/MCCM.html, ftp://ftp.ma.man.ac.uk/pub/narep.

Bélair, J. (1991). Population Models with State-Dependent Delays. In Arino, O., Axelrod, D. E., & Kimmel, M. (Eds.), *Mathematical Population Dynamics — Proceedings of the Second International Conference*, chap. 11, pp. 165–176. Marcel Dekker, Inc.

Bellman, R. E., & Cooke, K. L. (1963). *Differential-Difference Equations.* Academic Press.

Busenberg, S., & Cooke, K. L. (1980). The Effects of Integral Conditions in Certain Equations Modelling Epidemics and Population Growth. *J. Math. Biol.*, *10*, 13–32. Cited in Bélair (1991).

Clutter, J. L., Fortson, J. C., Pienaar, L. V., Brister, G. H., & Bailey, R. L. (1983). *Timber Management: A Quantitative Approach.* Wiley, London.

Cooke, K. L., & Yorke, J. A. (1973). Some Equations Modelling Growth Processes and Epidemics. *Math. Biosci.*, *16*, 75–101. Cited in Bélair (1991).

Driver, R. D. (1977). *Ordinary and Delay Differential Equations.* Springer-Verlag, New York.

El'sgol'ts, L. E., & Norkin, S. B. (1973). *Introduction to the Theory and Applications of Differential Equations with Deviating Arguments.* Academic Press, New York.

Faustmann, M. (1849). Berechnung des Wertes welchen Walboden sowie noch nicht haubare Holzbestände für die Waldwirtschaft besitzen. *Allgemeine Forst- und Jagd-Zeitung, 15.* (English translation in *Journal of Forest Economics 1*(1), 7–44, 1995).

García, O. (1990). Linear Programming and related approaches in Forest Planning. *New Zealand Journal of Forestry Science, 20*, 307–331.

Hale, J. K. (1977). *Functional Differential Equations.* Springer-Verlag, New York.

Hamming, R. W. (1962). *Numerical Methods for Scientists and Engineers.* McGraw-Hill, New York.

James, R. C. (1992). *Mathematics Dictionary* (5th edition). Chapman & Hall, New York.

Johansson, P., & Lofgren, K. (1985). *The Economics of Forestry and Natural Resources.* Blackwell, New York.

Kolmanovskii, V. B., & Myshkis, A. (1992). *Applied Theory of Functional Differential Equations.* Kluwer.

Kuang, Y. (1993). *Delay Differential Equations with Applications in Population Dynamics.* Academic Press.

Leuschner, W. A. (1990). *Forest Regulation, Harvest Scheduling, and Planning Techniques.* Wiley, New York.

Padulo, L., & Arbib, M. A. (1974). *System Theory.* Hemisphere Pub. Co., Washington, D.C.

Petrovski, I. G. (1971). *Lecciones de Teoría de las Ecuaciones Integrales.* Mir, Moscow.